

Sink Strength Dynamics Based on Potential Growth and Carbohydrate Accumulation in Strawberry Fruit

Hiromi Nakai

Graduate School of Bioresource and Bioenvironment Sciences, Kyushu University, 744 Motoooka, Nishi-ku, Fukuoka 819-0395, Japan

Daisuke Yasutake

Faculty of Agriculture, Kyushu University, 744 Motoooka, Nishi-ku, Fukuoka 819-0395, Japan; and IoP Collaborative Creation Center, Kochi University, 200, Otsu, Monobe, Nankoku, Kochi 783-8502, Japan

Kota Hidaka

Kyushu Okinawa Agricultural Research Center, National Agriculture and Food Research Organization, Kurume, Fukuoka 839-8503, Japan

Yuta Miyoshi

Takasaki Advanced Radiation Research Institute, National Institutes for Quantum and Radiological Science and Technology, 1233 Watanuki, Takasaki, Gunma 370-1292, Japan

Toshihiko Eguchi

Environmental Control Center for Experimental Biology, Kyushu University, 744 Motoooka, Nishi-ku, Fukuoka 819-0395, Japan

Gaku Yokoyama and Tomoyoshi Hirota

Faculty of Agriculture, Kyushu University, 744 Motoooka, Nishi-ku, Fukuoka 819-0395, Japan

Keywords. absolute growth rate, *Fragaria ×ananassa*, growth analysis, potential growth, relative growth rate

Abstract. Fruit size and sugar content are key determinants of fruit quality, influenced by environmental factors and agronomic practices and sink strength provided by the genetic potential. Strawberry (*Fragaria ×ananassa*) produces fruits arranged in inflorescences, whose growth is affected by carbon competition between them. The competitive ability is termed as sink strength, which can be quantified as the potential growth rate under sufficient resource supply and/or no carbon competition among sinks, referred to as non-limiting conditions. Most previous studies did not observe potential growth, thereby failing to adequately evaluate sink strength and to assess the influence of environmental factors and agronomic practices on fruit growth. This study aimed to investigate the potential growth of strawberry fruits and analyze its sink strength dynamics. Non-limiting conditions were established by removing flowers to one fruit per inflorescence in a greenhouse experiment with plants grown in soil and given water and nutrients through drip irrigation. Fruits were harvested every 5 days from 5 to 55 days after anthesis (DAA), measuring the size, weight, and concentrations of major soluble carbohydrates in strawberry (sucrose, glucose, and fructose) and starch. Sink strength was represented by absolute growth rate based on fruit weight, and its components, sink size and sink activity, were represented by weight and relative growth rate, respectively. Fruit volume and weight showed a gradual linear increase at 5 DAA and then rapidly increased, following a single sigmoid curve between 30 and 55 DAA. Fruits primarily accumulated glucose and fructose during early growth, shifting to sucrose after 35 DAA. Starch concentration peaked at 5 DAA and then exponentially decreased. Sink strength exhibited a single peak between 40 DAA and 45 DAA. Sink strength gradually increased with sink size until 30 DAA, whereas sink activity significantly decreased until 30 DAA. Thereafter, sink strength and sink activity exhibited a peak, whereas sink size continued to increase. These results suggest that the major determinant of sink strength was sink size during early fruit growth, shifting to sink activity during late growth.

Strawberry (*Fragaria ×ananassa* Duch.) is among the most popular and high-valued fruit crops because of its taste, flavor, and abundant nutritional value (Giampieri et al.

2012). Fruit size and sugar contents are major determinants of fruit quality (Basson et al. 2010; Lee et al. 2018). These characteristics change during fruit growth and ripening, and

they are primarily determined by the genotype but can also be influenced by the environment and agronomic management (Gündüz and Özdemir 2014).

Fruit growth largely depends on carbon and water accumulation. In other words, final fruit size and sugar content are determined by the availability of these resources. Carbon availability for fruit growth strongly relies on photosynthesis in source leaves and slightly on fruit respiration and photosynthesis (Blanke 2002), and these processes are influenced by environmental conditions such as light intensity, air temperature, and ambient CO₂ concentration (Hidaka et al. 2013; Sun et al. 2012). Water availability depends on the balance between water uptake, which is influenced by soil water content, and water loss through fruit transpiration, which is affected by air vapor pressure deficit. Thus, individual fruits achieve their genetically determined potential growth only under sufficient resource supply and optimal environmental conditions. Several studies have reported that fruits grown under resource-limited conditions, such as insufficient light, water stress, and high salinity showed decreased growth rate and quality (e.g., water content and fresh weight) compared with those grown under favorable conditions (Krauss et al. 2006; Mitchell et al. 1991; Morandi et al. 2011).

Furthermore, carbon availability for individual fruit growth is influenced not only by supply from the source but also by competition among sinks (Blanke 2009; Ho 1984). When the sink demand for carbon exceeds the supply from the source, carbon is unevenly distributed among sinks. As a result, there is a reduction in carbon import into fruits, which cannot achieve their potential growth. In many fruit crops, such as apple, tomato, and peach, flower and fruit thinning has been reported to improve the quality (e.g., size and weight) of remaining fruits (Link 2000). Therefore, because there is a tradeoff between fruit numbers and quality, it is necessary to properly manage their balance to improve profitability in fruit production.

The competitive ability of a sink to import carbon is defined as “sink strength” (Ho 1988). Fruit sink strength can be quantified as the potential growth rate corresponding to carbon import rate under non-limiting conditions, which is generally achieved by increasing photosynthesis and/or reducing fruit numbers to minimize competition (Dejong and Grossman 1995; Li et al. 2015; Marcelis 1996). Sink strength has been defined as the product of sink size and sink activity, which is generally stated as fruit fresh/dry weight and relative growth rate. Ho (1988) instead proposed a more physiological approach that sink size reflects physical constraints such as cell number, while sink activity reflects physiological processes such as phloem transport, metabolism, and imported sugar compartmentation. However, several studies suggested that cell number was not dominant of fruit size. Although there is a debate about a suitable measure of sink size and activity because the mechanisms to determine sink strength are unclear (Marcelis 1996; Rosati et al. 2020), the

former is practical because of its ease of measurement.

Sink strength varies during fruit growth; therefore, it has been used as a parameter in fruit growth models (Heuvelink 1999; Vos et al. 2010; Zhu et al. 2019). These models used potential growth rate as a determinant of sink strength to simulate carbon partitioning among fruits. They are useful to understand the way in which environment factors and agronomic practices can influence each fruit's growth, as well as to support decision-making in environmental control and agronomic practices.

Strawberry is a model fleshy fruit crop and a short-day plant, with its fruit consisting of the receptacle and the achene. The fruits are arranged in branched clusters known as inflorescences. They are classified as non-climacteric, and the major soluble carbohydrates contained in the fruit are sucrose, glucose, and fructose (Forney and Breen 1986). Starch is present only during early growth and almost disappears before ripening (Souleyre et al. 2004). In strawberry, similar to other fruit crops, resource-limited conditions, such as light (Hidaka et al. 2012; Watson et al. 2002) and water (Liu et al. 2007) deficits, lead to a decrease in fruit growth and quality. Furthermore, carbon isotope studies have suggested that fruits within a given inflorescence compete for carbon and fruit sink strength changes during growth and varies depending on inflorescence position (Hidaka et al. 2019; Miyoshi et al. 2021; Nishizawa and Hori 1988). However, most previous studies were performed in the presence of multiple fruits, thus they did not observe the potential growth. Because fruit growth in these studies results from carbon competition, they are insufficient to discuss changes in sink strength with fruit growth. To our knowledge, the study by Miura et al. (1990) is the only study that investigated fruit growth with one fruit per inflorescence; however, they discussed the growth rate based on fruit length rather than weight, which does not directly assess carbon accumulation.

This study aimed 1) to investigate the potential growth of strawberry fruits and 2) to analyze sink strength dynamics based on fruit weight. Information on potential growth will

lay a foundation for the study of strawberry fruit growth, as well as for appropriate environmental control and agronomic practices aimed at enhancing strawberry productivity. In this study, potential growth under non-limiting conditions was evaluated following removing flowers to achieve one fruit per inflorescence.

Materials and Methods

Plant materials and growth conditions. Strawberry plants (*Fragaria ×ananassa* Duch. 'Fukuoka S6') were grown under natural light in a greenhouse (20 m long × 8 m wide × 4 m high) at Ito Plant Experiment Fields & Facilities, Faculty of Agriculture, Kyushu University, Japan (lat. 33°59.3'N, long. 130°21.5'E). On 27 and 28 Sep 2022, nursery plants were transplanted into cultivation beds (9.7 m long × 0.3 m wide × 0.12 m high) filled with commercial soil mixture ICHIGO BAIDO (Green Sangyo Co. Ltd., Saga, Japan). A total of 141 plants were planted in two rows, with a separation of 0.2 m between plants and 0.18 m between rows. A nutrient solution (OK-F-1, OAT Agrio Co., Ltd., Tokyo, Japan; 75N-40P-85K mg·L⁻¹) adjusted to an electrical conductivity of 0.6 dS·m⁻¹ was automatically supplied at a rate of 200 mL·d⁻¹ per plant using a drip irrigation system. The air temperature in the greenhouse was kept at 8 to 22 °C using a heater and natural ventilation through the roof and side windows.

To establish non-limiting conditions for evaluating potential growth, the first flower on the primary inflorescence of each plant was hand-pollinated at anthesis, and subsequent flowers were removed before anthesis. Each plant had eight fully expanded leaves during the experiments.

Measurement of environmental conditions. Inside the greenhouse, air temperature and relative humidity and photosynthetic photon flux density (PPFD) were measured using a temperature-humidity sensor (HMP60; Vaisala, Vantaa, Finland) installed in a forced ventilation shelter (RSVH01A1203; SCE, Inc., Hokkaido, Japan) and a light quantum meter (PAR-02D; Prede Co., Ltd., Tokyo, Japan), respectively. Sensors were located at the center of the cultivation beds at a height of 1.2 m (near the top of the canopy). Data were measured at 5-s intervals, and 5-min means were automatically stored using a data logger (CR1000; Campbell Scientific, Logan, UT, USA). Daily averaged air temperature and relative humidity and daily cumulative PPFD were calculated in R version 4.3.1 (R Core Team 2023).

Fruit harvest. A total of 141 flowers that bloomed between 19 and 30 Nov 2022, were tagged at anthesis, and the fruit growth stage was identified as the number of days after anthesis (DAA). Fruits were harvested at 11 different growth stages: 5, 10, 15, 20, 25, 30, 35, 40, 45, 50, and 55 DAA. For each stage, 12 to 14 fruits were collected, and growth characteristics were measured. Each fruit served as a biological replicate.

Measurements of parameters related to fruit size and weight. Immediately following harvest, the dimensions of the major axis

(length: L , mm), medium axis (width: W , mm), and minor axis (thickness: T , mm) of fruits were measured using a digital caliper (E05-150 130-720; As-One Co., Osaka, Japan) after removing the calyx. Fruit volume was estimated using the following equation:

$$V = 4.0 * (L * W * T * 10^{-4}) + 2.0724,$$

where V is fruit volume (cm³). The equation was elaborated based on the same cultivar used in this study (data not shown). The fresh weight (FW, g) of each fruit was measured, followed by cutting into small pieces and immediate freezing in liquid nitrogen. The frozen samples were ground to fine powder with liquid nitrogen using a mortar and pestle or a cool mill (TK-CM20S; Tokken, Chiba, Japan), followed by storage at -80 °C for further analysis. Fruit dry weight (DW, g) was calculated based on dry matter percentages obtained by the lyophilization of pre-weighted frozen powder and measured FW values. Fruit water content (FWC, %) was calculated based on the difference between FW and DW as follows:

$$FWC = (FW - DW) / FW * 100$$

Fruit carbohydrate analysis. In this study, to investigate carbon accumulation during fruit growth, the concentrations based on FW and contents in whole fruits of the major soluble carbohydrates (sucrose, glucose, and fructose) and starch in strawberry fruits were analyzed.

Soluble carbohydrates were extracted following the procedures described in Souleyre et al. (2004) with some modifications, and concentrations were determined using high-performance liquid chromatography (HPLC) analysis (Nakai et al. 2022). Approximately 20 mg of fruit frozen powder was weighted and extracted in 0.8 mL 80% (v/v) ethanol at 82 °C for 5 min. The extract was centrifuged for 10 min at 20,630 g_n at room temperature for 10 min and re-extracted four times using 0.6 mL 80% (v/v) ethanol at 82 °C for 5 min. The supernatant was pooled and evaporated to dryness, and the residue was dissolved in 3.2 mL of distilled water. The solution was centrifuged at 20,630 g_n and 4 °C for 5 min, and the supernatant was filtered through a 0.45- μ m membrane filter and used for HPLC analysis. The HPLC system (Shimadzu Corp., Kyoto, Japan) consisted of a DGU-20A3 on-line degassing unit, an LC-20AD pump unit, an SIL-20A auto-sampler, an RID-10A refractive index detector, a CTO-20A column oven, and a Shim-pack SCR-101N column (300 mm × 7.9 mm i.d., 10 μ m). LC-Solution software (Shimadzu Corp., Kyoto, Japan) was used for controls and data acquisition. The mobile phase was distilled water at a flow rate of 0.7 mL·min⁻¹ at 40 °C, and the injection volume was 20 μ L. Starch concentration was determined using a Total Starch Assay kit (K-TSTA, Megazyme, Bray, Ireland) enzymatic assay following to the manufacturer's protocol with slight modifications. Following ethanol extraction, tissue pellets were re-suspended in 1 mL of sodium acetate (100 mM, pH 5.0) and starch was converted to glucose by the addition of 10 μ L each of α -amylase (2500 U·mL⁻¹)

Received for publication 13 Jun 2024. Accepted for publication 24 Jul 2024.

Published online 13 Sep 2024.

This study was financially supported by Grant-in-Aid for JSPS Fellows (JSPS KAKENHI Grant Number JP23KJ1707); JST SPRING (Grant Number JPMJSP2136); Cabinet Office grant-in-aid, the Advanced Next-Generation Greenhouse Horticulture by IoP (Internet of Plants), Japan; Cabinet Office grant-in-aid "Evolution to Society 5.0 Agriculture Driven by IoP (Internet of Plants)," Japan; and Grant-in-Aid for Scientific Research (JSPS KAKENHI Grant Number JP23H02342).

D.Y. is the corresponding author. E-mail: yasutake@bpes.kyushu-u.ac.jp.

This is an open access article distributed under the CC BY-NC license (<https://creativecommons.org/licenses/by-nc/4.0/>).

and amyloglucosidase (3300 U·mL⁻¹). Samples were centrifuged at 15,500 g_n for 5 min at room temperature, and 50 μL of the supernatant was incubated with 1.5 mL of Megazyme GOPOD reagent. Glucose released from starch was then spectrophotometrically quantified at 510 nm. For carbohydrate analysis, two technical replicates were analyzed per biological replicate. Whole-fruit contents were calculated by multiplying the concentration based on FW by the FW. For comparison purposes, carbohydrate concentrations and contents were expressed as moles of carbon.

Assuming that carbon imported into the fruits, except for that consumed in respiration, was distributed among sucrose, glucose, fructose, starch, and other carbon compounds, the relative distribution of carbon was determined by dividing the accumulation rate of each component by that of total carbon contents. The total carbon content was calculated by multiplying the DW by the amount of carbon per unit gram of DW (0.45 g C/g DW), which was an average value calculated from literature data of various species (Cakpo et al. 2020). The content of the other carbon compounds was calculated by subtracting the contents of the four aforementioned carbohydrates from the total carbon content.

Fruit growth analysis. As reported by Roch et al. (2020), the time courses of FW and DW were, after log transformation, fitted to double sigmoid functions by the least square methods using Broyden-Fletcher-Goldfarb-Shanno algorithm implemented by the *optim* function of the R stats package (R Core Team 2023). These fitting parameters were used to calculate the absolute growth rate (AGR) and relative growth rate (RGR) based on FW and DW. AGR was obtained as the first derivative of the double sigmoid functions. RGR was calculated by dividing AGR by FW or DW.

Statistical analyses. All statistical analyses were performed in R version 4.3.1 (R Core Team 2023) in the RStudio environment (version 2023.06.0) (RStudio Team 2023). In Figs. 2–4, data were statistically expressed as means ± SE (n = 12 to 14). Where the error bars are not visible, the standard error was smaller than the plotting symbol.

Results

Environmental conditions. Daily averaged air temperature during the growth period gradually decreased, despite remaining above the heater threshold temperature (8°C) (Fig. 1A). Daily averaged relative humidity stayed within the range of 51% to 98% (Fig. 1B). Daily cumulative PPFD exhibited significant fluctuations throughout the experimental period, with a maximum of approximately 12.6 mol·m⁻²·d⁻¹ and a minimum of 1.5 mol·m⁻²·d⁻¹ (Fig. 1C).

Fruit dimensions and volume. The three dimensions of fruit followed a double sigmoid curve with two rapid growth periods (5 to 20 DAA and 30 to 45 DAA) (Fig. 2A). The length was always longer than the width and the thickness and continued to increase until 55 DAA, while the width and the thickness similarly increased and reached a plateau at 45 DAA. The volume immediately

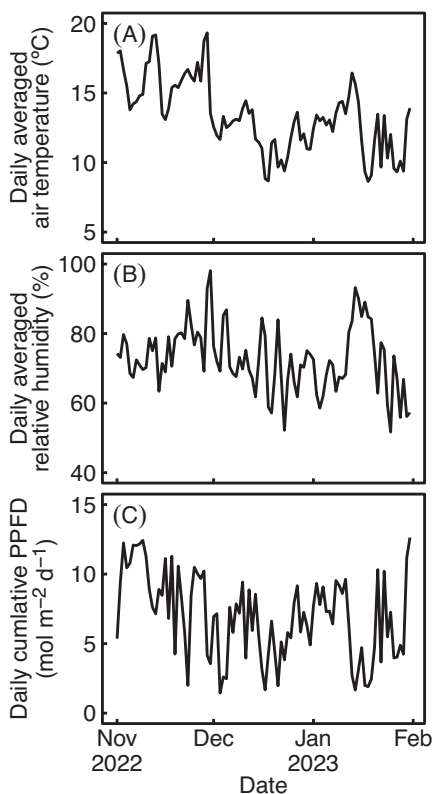


Fig. 1. Changes in daily averaged air temperature (A) and relative humidity (B) and daily cumulative photosynthetic photon flux density (PPFD) (C) measured in the greenhouse throughout the experimental period (11 Nov 2022 to 31 Jan 2023).

after anthesis (5 DAA) was approximately 2.3 cm³ (Fig. 2B). Subsequently, the volume increased linearly until 30 DAA, and then it followed a single sigmoid curve, reaching approximately 37.5 cm³ at 55 DAA.

Fruit weight and water content. The changes in FW and DW showed a similar pattern to the volume (Fig. 3A). FW began to show a gradual linear increase from approximately 0.2 g at 5 DAA, and then rapidly increased to approximately 35 g, following a single sigmoid curve between 30 and 55 DAA. DW was approximately 0.04 g at 5 DAA, and then increased to approximately 4.4 g, following a single sigmoid curve after the linear increase. FWC increased from approximately 78.5% to 90.0%, peaking at 40 DAA, and then decreasing to approximately 87.3% (Fig. 3B).

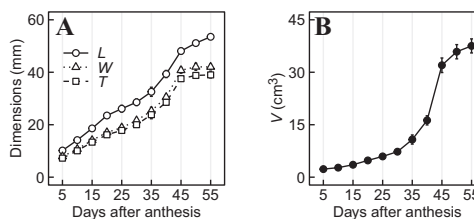


Fig. 2. Changes in fruit dimensions based on length (L; opened circles), width (W; opened triangles), and thickness (T; opened squares) (A) and fruit volume (V) (B). Error bars represent the standard error of the mean values (n = 12 to 14).

Fruit carbohydrate concentrations and contents. Sucrose concentration remained almost constant between 5 DAA and 30 DAA with only an increase of approximately 4 μmol C/g FW but increased to 1400 μmol C/g FW, following a single sigmoid curve, from 30 DAA (Fig. 4A). Contrastingly, glucose concentration did not exhibit a rapid increase, and it linearly increased until 35 DAA and then increased slightly faster to 830 μmol C/g FW. Fructose concentration increased to 810 μmol C/g FW, following a similar pattern to that of glucose. The starch concentration at 5 DAA was approximately 280 μmol C/g FW, similar to that of the other three carbohydrates, but then exponentially decreased and was below the detection limit after 45 DAA.

Sucrose, glucose, and fructose contents increased following a single sigmoid curve, but starch contents remained almost constant at 0.1 mmol C per fruit until 45 DAA, reaching values below the detection limit after this point (Fig. 4B).

Accumulation rate and relative distribution ratio of carbon. Both the accumulation rate of sucrose, glucose, fructose, starch, and other carbon compounds (Fig. 5A) and the relative distribution of imported carbon between them (Fig. 5B) changed depending on fruit growth. At the early growth stage, other carbon compounds accumulated more notably than soluble carbohydrates and starch, with more than 70% of the imported carbon distributed to them. With fruit growth, accumulation of soluble carbohydrates increased, with more than 50% of the imported carbon distributed to them after 25 DAA. Although there were few changes in relative distributions between 25 DAA and 35 DAA and between 35 DAA and 50 DAA, accumulation rates varied. All except for starch were predominantly accumulated between 40 DAA and 45 DAA. At the end of growth, most of the carbon imported into the fruits was distributed to soluble carbohydrates.

Fruit growth rate. Fruit growth rate was calculated based on daily changes in FW and DW estimated by parameter fitting. A double sigmoid curve was fitted well to both log-transformed FW and log-transformed DW (Fig. 6). Both AGR and RGR exhibited similar patterns based on FW and DW (Fig. 7). AGR began to gradually increase during early growth, increasing rapidly from 30 DAA, peaking at between 40 DAA and 45 DAA, and then exponentially decreasing until 55 DAA. RGR was

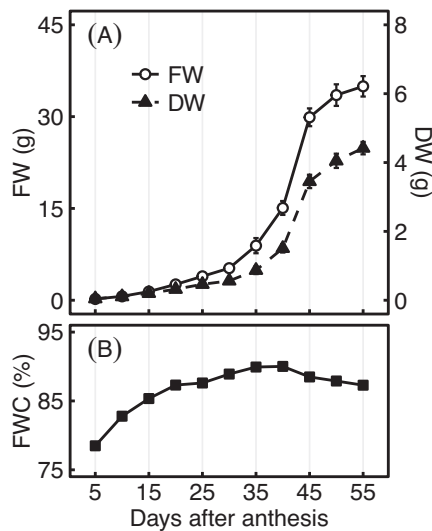


Fig. 3. Changes in fruit fresh weight (FW; opened circles), dry weight (DW; closed triangles) (A), and fruit water content (FWC) (B). Error bars represent the standard error of the mean values ($n = 12$ to 14).

high during early growth, decreasing until 30 DAA, then increasing again to the same level as that in the early stage, and peaking at around 40 DAA.

Discussion

Fruit growth pattern. Previous studies have demonstrated that the growth of strawberry fruits follows either a single sigmoid or double sigmoid curve in different cultivars (Menzel 2023; Perkins-Veazie and Huber 1987). Miura et al. (1990) and Li et al. (2012) reported a double sigmoid curve for fruit diameter in 'Reiko' and 'Akihime', respectively. Pei et al. (2020) identified a double sigmoid curve for fruit FW in 'Hongyan', and Symons et al. (2012) showed a single sigmoid curve for both diameter and FW in 'Red Gauntlet'. In this study, we showed a double sigmoid curve for diameter (Fig. 2) and a single sigmoid curve after a linear increase for volume (Fig. 2), FW, and DW (Fig. 3) in 'Fukuoka S6'.

Fruit growth patterns are typically characterized by an initial phase of intense cell division and followed by a cell expansion phase.

In strawberry, fruits grow slowly during the cell division phase for 15 to 20 DAA and then grow to their mature size during the cell expansion phase (Menzel 2023). Pei et al. (2020) measured fruit FW, cell size, and cell number during growth in 'Hongyan' and found that they followed a double sigmoid curve after the cell division phase. The results of the present study, in which FW increased linearly until 30 DAA and then followed a single sigmoid curve, suggested that in 'Fukuoka S6' fruit exhibiting potential growth, the cell division phase continued for approximately 30 d and then shifted to the cell expansion phase.

Carbon accumulation and relative distribution ratio. In strawberry, carbon is translocated from leaves to fruits as sucrose (Forney and Breen 1985), which is then converted into other carbohydrates or carbon compounds. As mentioned earlier, strawberry fruits primarily accumulate sucrose, glucose, and fructose, and their composition varies depending on cultivars and growth stages (Fait et al. 2008; Sturm et al. 2003). In this study, sucrose concentration was lower than glucose and fructose concentrations during the early growth stage, although it increased more rapidly and surpassed them during development (Fig. 4A). These findings are consistent with those of previous studies conducted on other cultivars without fruit removal (e.g., Jia et al. 2013; Luo et al. 2020). However, sucrose concentration declined more dramatically than glucose and fructose concentrations when carbohydrate levels decreased overall under resource-limited conditions because of insufficient sunlight (Liu et al. 2020). Hence, the accumulation pattern of these three carbohydrates may be different depending on whether the fruit achieves its potential growth.

Starch concentrations continued to decrease from 5 DAA, reaching non-detectable levels at 45 DAA (Fig. 4A). Starch concentrations were reported to decrease by half between 7 DAA and 14 DAA, being barely detectable after 31 DAA (Souleyre et al. 2004). Starch accumulation patterns in fruits exhibiting potential growth determined in this study match previously observed values. Contrary to expectation, starch content was practically constant throughout development (Fig. 4B), suggesting that the decrease in starch concentration was due to a dilution caused by fruit volumetric growth rather than starch degradation. However, because it has been observed

that starch granules in 70% to 80% of the cells examined in ripe fruits were lost (Knee et al. 1977; Souleyre et al. 2004), the detection accuracy in this study might have been insufficient to assess low starch concentrations.

Furthermore, this study found that the distribution of carbon imported into fruits to other compounds was equal or greater than its distribution to the major carbon compounds in fruits (sucrose, glucose, fructose, starch) during most stages of growth. These other compounds notably accumulated between 40 to 45 DAA (Fig. 5A), when fruit volume rapidly increased (Fig. 2). Our results suggest that the other carbon compounds were mainly cell wall materials such as cellulose (Taiz et al. 2015).

The results of carbon accumulation rate and relative distribution ratio (Fig. 5) would reflect sugar metabolism and unloading in strawberry fruit. Further research on enzymes related to these processes would be useful to elucidate the physiological mechanism determining sink strength (Yamaki 2010).

Sink strength. Sink strength has been proposed to depend on sink size and sink activity, as described previously. In this study, we quantified sink strength as the AGR of a fruit exhibiting potential growth, sink size as fruit weight, and sink activity as the RGR. Until 30 DAA, both sink strength and sink size gradually increased, while sink activity greatly decreased (Figs. 3 and 7). Subsequently, sink strength and sink activity exhibited a peak, whereas sink size continued to increase. Although several studies have argued that sink activity, rather than sink size, affects sink strength (Hidaka et al. 2019; Marcelis 1996), our results suggested that the major determinant of sink strength was sink size during early fruit growth, changing to sink activity during late growth. Although this study assessed sink size and sink activity by the practical approach (i.e., fruit weight and RGR), further elucidation of the mechanisms to determine sink strength would benefit from the analysis of cell number and physiological processes.

The AGR pattern was consistent with that of other fruit species whose FW followed a single sigmoid curve (Roch et al. 2020). The AGR dynamics suggested that sink strength was altered during fruit development, reaching a maximum between 40 DAA and 45 DAA. Hidaka et al. (2019) implemented the carbon isotope tracer method to report that sink strength, represented by the carbon import rate into the fruit, was faster in white-colored fruits compared with green-colored fruits and fruits turning red. The color of strawberries changed from green to white in the early growth stage and then to red at maturity. In our study, strawberries were green at 5 to 30 DAA, white at 35 to 40 DAA, and turning red at 45 DAA. This slight discrepancy may be due to differences in the number and position of fruits on the inflorescence, which affect carbon partitioning among fruits. Although we followed the specific fruits exhibiting potential growth, Hidaka et al. (2019)

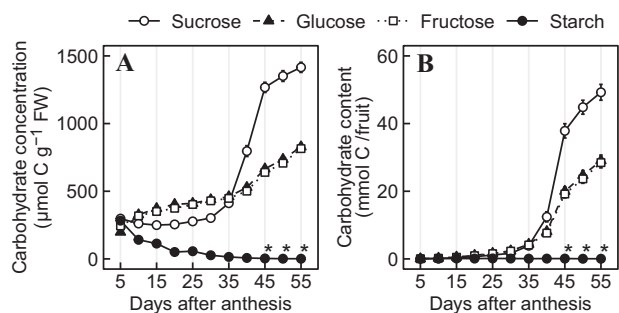


Fig. 4. Changes in concentrations (A) and contents (B) of sucrose (open circles), glucose (closed triangles), fructose (open squares), and starch (closed circles). Error bars represent the standard error of the mean values ($n = 12$ to 14). Values marked with an asterisk were below the detection limit.

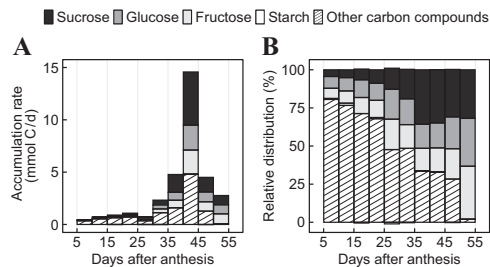


Fig. 5. Changes in the accumulation rate of sucrose, glucose, fructose, starch, and other carbon compounds (A) and their relative distribution ratios to the total carbon imported into the fruits (B).

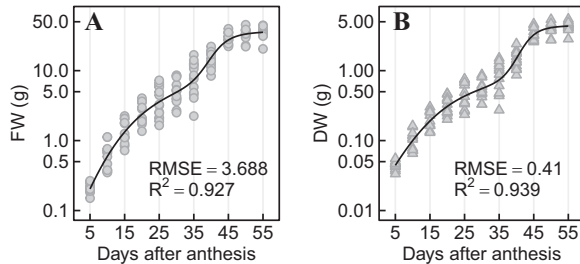


Fig. 6. Measured data (circles and triangles) of fresh weight (FW) (A) and dry weight (DW) (B), and their corresponding fitted curves (lines) on a log scale. The root mean squared error (RMSE) and the coefficient of determination (R^2) are shown.

compared different fruits on the inflorescence to assess changes in sink strength. In addition, growth conditions may have also affected the results, as they affect anthocyanin accumulation in fruits, and thus coloration (Ikeda et al. 2011; Zhang et al. 2018). Furthermore, the RGR based on both FW and DW showed a similar pattern to that based on fruit length reported by Miura et al. (1990). They also demonstrated that, although there were differences in peak position and value, the RGR based on the length of fruits exhibiting potential growth was similar to that of fruits impacted by carbon competition. Further studies with an increased focus on RGR peak position and value are required to evaluate the effects of carbon competition and environmental conditions on the sink activity of each fruit.

In addition, sink strength and carbon competition can vary among inflorescences. Strawberry plants continually produce multiple inflorescences, causing the environmental conditions to which the plants are exposed during fruit growth to change throughout the cultivation period. Environmental factors such as air temperature can affect sink activity, which reflects physiological processes in fruits. These factors also influence photosynthesis and, consequently, the carbon

supply to fruits. It has been reported that approximately 90% of the carbon supplied from source is distributed to fruits during the fruit growth period of the first inflorescence (Nishizawa and Hori 1988). However, carbon competition among fruits and/or other sinks may change if carbon availability varies. Therefore, future research on the difference in sink strength dynamics among inflorescences would be beneficial to provide a foundation for appropriate environmental control and agronomic practices aimed at enhancing long-term strawberry production.

Conclusion

The present study was designed to evaluate the growth characteristics of strawberry fruits exhibiting potential growth. Fruits under non-limiting conditions generated by flower removing exhibited a linear increase followed by a single sigmoid curve in both volume and weight. The relative distribution ratio of carbon imported into the fruits to soluble carbohydrates was low during early growth but increased with fruit growth. The accumulation pattern of carbohydrates was different between sucrose and hexose (i.e., glucose and fructose); hexose accumulated

faster than sucrose during early growth, and then sucrose accumulated markedly during development. Sink strength analyzed based on fruit weight appears to be strongly influenced by sink size during early growth but by sink activity during late growth. Further research is required to physiologically analyze the sink strength dynamics and to evaluate the effects of limitations such as carbon competition; however, the present study lays the groundwork for future research into strawberry fruit growth and contributes to the development of management strategies for environmental control and agronomic practices to enhance strawberry productivity.

References Cited

- Basson CE, Groenewald JH, Kossmann J, Cronjé C, Bauer R. 2010. Sugar and acid-related quality attributes and enzyme activities in strawberry fruits: Invertase is the main sucrose hydrolysing enzyme. *Food Chem.* 121(4):1156–1162. <https://doi.org/10.1016/j.foodchem.2010.01.064>.
- Blanke MM. 2002. Photosynthesis of strawberry fruit. *Acta Hort.* 567:373–376. <https://doi.org/10.17660/ActaHortic.2002.567.81>.
- Blanke MM. 2009. Regulatory mechanisms in source sink relationships in plants – A review. *Acta Hort.* 835:13–20. <https://doi.org/10.17660/ActaHortic.2009.835.1>.
- Cakpo CB, Vercambre G, Baldazzi V, Roch L, Dai Z, Valsesia P, Memah MM, Colombié S, Moing A, Gibon Y, Génard M. 2020. Model-assisted comparison of sugar accumulation patterns in ten fleshy fruits highlights differences between herbaceous and woody species. *Ann Bot.* 126(3):455–470. <https://doi.org/10.1093/aob/mcaa082>.
- Dejong TM, Grossman YL. 1995. Quantifying sink and source limitations on dry matter partitioning to fruit growth in peach trees. *Physiol Plant.* 95(3):437–443. <https://doi.org/10.1034/j.1399-3054.1995.950315.x>.
- Fait A, Hanhineva K, Beleggia R, Dai N, Rogachev I, Nikiforova VJ, Fernie AR, Aharoni A. 2008. Reconfiguration of the achene and receptacle metabolic networks during strawberry fruit development. *Plant Physiol.* 148(2):730–750. <https://doi.org/10.1104/pp.108.120691>.
- Forney CF, Breen PJ. 1985. Collection and characterization of phloem exudate from strawberry pedicels. *HortScience.* 20(3):413–414. <https://doi.org/10.21273/HORTSC.20.3.413>.
- Forney CF, Breen PJ. 1986. Sugar content and uptake in the strawberry fruit. *J Amer Soc Hort Sci.* 111(2):241–247. <https://doi.org/10.21273/JASHS.111.2.241>.
- Giampieri F, Tulipani S, Alvarez-Suarez JM, Quiles JL, Mezzetti B, Battino M. 2012. The strawberry: Composition, nutritional quality, and impact on human health. *Nutrition.* 28(1):9–19. <https://doi.org/10.1016/j.nut.2011.08.009>.
- Gündüz K, Özdemir E. 2014. The effects of genotype and growing conditions on antioxidant capacity, phenolic compounds, organic acid and individual sugars of strawberry. *Food Chem.* 155:298–303. <https://doi.org/10.1016/j.foodchem.2014.01.064>.
- Heuvelink E. 1999. Evaluation of a dynamic simulation model for tomato crop growth and development. *Ann Bot.* 83(4):413–422. <https://doi.org/10.1006/anbo.1998.0832>.
- Hidaka K, Dan K, Imamura H, Miyoshi Y, Takayama T, Sameshima K, Kitano M, Okimura M. 2013. Effect of supplemental lighting from different light sources on growth and yield of

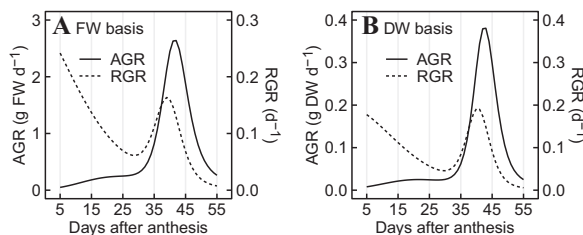


Fig. 7. Changes in absolute growth rate (AGR; solid line) and relative growth rate (RGR; dotted line) based on fresh weight (FW) (A) and dry weight (DW) (B).

- strawberry. *Environ Control Biol.* 51(1):41–47. <https://doi.org/10.2525/ecb.51.41>.
- Hidaka K, Ito E, Sago Y, Yasutake D, Miyoshi Y, Kitano M, Miyauchi K, Okimura M, Imai S. 2012. High yields of strawberry by applying vertically-moving beds on the basis of leaf photosynthesis. *Environ Control Biol.* 50(2):143–152. <https://doi.org/10.2525/ecb.50.143>.
- Hidaka K, Miyoshi Y, Ishii S, Suzui N, Yin YG, Kurita K, Nagao K, Araki T, Yasutake D, Kitano M, Kawachi N. 2019. Dynamic analysis of photosynthate translocation into strawberry fruits using non-invasive ^{11}C -labeling supported with conventional destructive measurements using ^{13}C -labeling. *Front Plant Sci.* 9(January):1946–1912. <https://doi.org/10.3389/fpls.2018.01946>.
- Ho LC. 1984. Partitioning of assimilates in fruiting tomato plants. *Plant Growth Regul.* 2(4):277–285. <https://doi.org/10.1007/BF00027287>.
- Ho LC. 1988. Metabolism and compartmentation of imported sugars in sink organs in relation to sink strength. *Annu Rev Plant Physiol Plant Mol Biol.* 39(1):355–378. <https://doi.org/10.1146/annurev.pp.39.060188.002035>.
- Ikeda T, Suzuki N, Nakayama M, Kawakami Y. 2011. The effects of high temperature and water stress on fruit growth and anthocyanin content of pot-grown strawberry (*Fragaria × ananassa* Duch. cv. ‘Sachinoka’) plants. *Environ Control Biol.* 49(4):209–215. <https://doi.org/10.2525/ecb.49.209>.
- Jia H, Wang Y, Sun M, Li B, Han Y, Zhao Y, Li X, Ding N, Li C, Ji W, Jia W. 2013. Sucrose functions as a signal involved in the regulation of strawberry fruit development and ripening. *New Phytol.* 198(2):453–465. <https://doi.org/10.1111/nph.12176>.
- Knee M, Sargent JA, Osborne DJ. 1977. Cell wall metabolism in developing strawberry fruits. *J Exp Bot.* 28(2):377–396. <https://doi.org/10.1093/jxb/28.2.377>.
- Krauss S, Schnitzler WH, Grassmann J, Woitke M. 2006. The influence of different electrical conductivity values in a simplified recirculating soilless system on inner and outer fruit quality characteristics of tomato. *J Agric Food Chem.* 54(2):441–448. <https://doi.org/10.1021/jf051930a>.
- Lee J, Kim HB, Noh YH, Min SR, Lee HS, Jung J, Park KH, Kim DS, Nam MH, Kim TI, Kim SJ, Kim HR. 2018. Sugar content and expression of sugar metabolism-related gene in strawberry fruits from various cultivars. *J Plant Biotechnol.* 45(2):90–101. <https://doi.org/10.5010/JPB.2018.45.2.090>.
- Li CL, Fang KF, Lei H, Xing Y, Shen YY. 2012. Phloem unloading follows an extensive apoplastic pathway in developing strawberry fruit. *J Horticult Sci Biotechnol.* 87(5):470–477. <https://doi.org/10.1080/14620316.2012.11512897>.
- Li T, Heuvelink E, Marcelis LFM. 2015. Quantifying the source-sink balance and carbohydrate content in three tomato cultivars. *Front Plant Sci.* 6(June):416–410. <https://doi.org/10.3389/fpls.2015.00416>.
- Link H. 2000. Significance of flower and fruit thinning on fruit quality. *Plant Growth Regul.* 31(1–2):17–26. <https://doi.org/10.1023/a:1006334110068>.
- Liu F, Savić S, Jensen CR, Shahnazari A, Jacobsen SE, Stikić R, Andersen MN. 2007. Water relations and yield of lysimeter-grown strawberries under limited irrigation. *Sci Hortic.* 111(2):128–132. <https://doi.org/10.1016/j.scienta.2006.10.006>.
- Liu HT, Ji Y, Liu Y, Tian SH, Gao QH, Zou XH, Yang J, Dong C, Tan JH, Ni DA, Duan K. 2020. The sugar transporter system of strawberry: Genome-wide identification and expression correlation with fruit soluble sugar-related traits in a *Fragaria × ananassa* germplasm collection. *Hortic Res.* 7(1): <https://doi.org/10.1038/s41438-020-00359-0>.
- Luo J, Peng F, Zhang S, Xiao Y, Zhang Y. 2020. The protein kinase FaSnRK1 α regulates sucrose accumulation in strawberry fruits. *Plant Physiol Biochem.* 151:369–377. <https://doi.org/10.1016/j.plaphy.2020.03.044>.
- Marcelis LFM. 1996. Sink strength as a determinant of dry matter partitioning in the whole plant. *J Exp Bot.* 47(Special_Issue):1281–1291. https://doi.org/10.1093/jxb/47.Special_Issue.1281.
- Menzel C. 2023. A review of fruit development in strawberry: High temperatures accelerate flower development and decrease the size of the flowers and fruit. *J Horticult Sci Biotechnol.* 98(4):409–431. <https://doi.org/10.1080/14620316.2023.2166599>.
- Mitchell JP, Shennan C, Grattan SR. 1991. Developmental changes in tomato fruit composition in response to water deficit and salinity. *Physiol Plant.* 83(1):177–185. <https://doi.org/10.1111/j.1399-3054.1991.tb01299.x>.
- Miura H, Imada S, Yabuuchi S. 1990. Double sigmoid growth curve of strawberry fruit. *Engei Gakkai Zasshi.* 59(3):527–531. <https://doi.org/10.2503/jjshs.59.527>.
- Miyoshi Y, Hidaka K, Yin YG, Suzui N, Kurita K, Kawachi N. 2021. Non-invasive ^{11}C -Imaging revealed the spatiotemporal variability in the translocation of photosynthates into strawberry fruits in response to increasing daylight integrals at leaf surface. *Front Plant Sci.* 12(July):688887. <https://doi.org/10.3389/fpls.2021.688887>.
- Morandi B, Zibordi M, Losciale P, Manfrini L, Pierpaoli E, Grappadelli LC. 2011. Shading decreases the growth rate of young apple fruit by reducing their phloem import. *Sci Hortic.* 127(3):347–352. <https://doi.org/10.1016/j.scienta.2010.11.002>.
- Nakai H, Yasutake D, Kimura K, I K, Hidaka K, Eguchi T, Hirota T, Okayasu T, Ozaki Y, Kitano M. 2022. Dynamics of carbon export from leaves as translocation affected by the coordination of carbohydrate availability in field strawberry. *Environ Exp Bot.* 196(February):104806. <https://doi.org/10.1016/j.envexpbot.2022.104806>.
- Nishizawa T, Hori Y. 1988. Translocation and distribution of ^{14}C -photoassimilates in strawberry plants varying in developmental stages of the inflorescence. *Engei Gakkai Zasshi.* 57(3):433–439. <https://doi.org/10.2503/jjshs.57.433>.
- Pei MS, Cao SH, Wu L, Wang GM, Xie ZH, Gu C, Zhang SL. 2020. Comparative transcriptome analyses of fruit development among pears, peaches, and strawberries provide new insights into single sigmoid patterns. *BMC Plant Biol.* 20(1):108–115. <https://doi.org/10.1186/s12870-020-2317-6>.
- Perkins-Veazie P, Huber DJ. 1987. Growth and ripening of strawberry fruit under field conditions. *Proc Fla State Hortic Soc.* 100:253–256. <https://doi.org/10.1002/9780470650585.ch8>.
- R Core Team. 2023. R-4.3.1 for macOS. R Foundation for Statistical Computing, Vienna, Austria. <https://www.r-project.org/>. [accessed 27 Mar 2024].
- R Studio Team. 2023. RStudio: Integrated development for R. RStudio, PBC, Boston, MA. <http://www.rstudio.com/>. [accessed 27 Mar 2024].
- Roch L, Prigent S, Klose H, Cakpo CB, Beauvoit B, Deborde C, Fouillen L, Van Delft P, Jacob D, Usadel B, Dai Z, Génard M, Vercambre G, Colombié S, Moing A, Gibon Y. 2020. Biomass composition explains fruit relative growth rate and discriminates climacteric from non-climacteric species. *J Exp Bot.* 71(19):5823–5836. <https://doi.org/10.1093/jxb/era302>.
- Rosati A, Caporali S, Hammami SBM, Moreno-Alías I, Rapoport H. 2020. Fruit growth and sink strength in olive (*Olea europaea*) are related to cell number, not to tissue size. *Funct Plant Biol.* 47(12):1098–1104. <https://doi.org/10.1071/FP20076>.
- Souleyre EJF, Iannetta PPM, Ross HA, Hancock RD, Shepherd LVT, Viola R, Taylor MA, Davies HV. 2004. Starch metabolism in developing strawberry (*Fragaria × ananassa*) fruits. *Physiol Plant.* 121(3):369–376. <https://doi.org/10.1111/j.0031-9317.2004.0338.x>.
- Sturm K, Koron D, Stampar F. 2003. The composition of fruit of different strawberry varieties depending on maturity stage. *Food Chem.* 83(3):417–422. [https://doi.org/10.1016/S0308-8146\(03\)00124-9](https://doi.org/10.1016/S0308-8146(03)00124-9).
- Sun P, Mantri N, Lou HQ, Hu Y, Sun D, Zhu YQ, Dong TT, Lu HF. 2012. Effects of elevated CO $_2$ and temperature on yield and fruit quality of strawberry (*Fragaria × ananassa* Duch.) at two levels of nitrogen application. *PLoS One.* 7(7):e41000. <https://doi.org/10.1371/journal.pone.0041000>.
- Symons GM, Chua Y-J, Ross JJ, Quittenden LJ, Davies NW, Reid JB. 2012. Hormonal changes during non-climacteric ripening in strawberry. *J Exp Bot.* 63(13):4741–4750. <https://doi.org/10.1093/jxb/ers147>.
- Taiz L, Zeiger E, Moller IM, Murphy A. 2015. Plant physiology and development (6th ed). Sinauer Associates, Sunderland, MA, USA.
- Vos J, Evers JB, Buck-Sorlin GH, Andrieu B, Chelle M, De Visser PHB. 2010. Functional-structural plant modelling: A new versatile tool in crop science. *J Exp Bot.* 61(8):2101–2115. <https://doi.org/10.1093/jxb/erp345>.
- Watson R, Wright CJ, McBurney T, Taylor AJ, Linforth RST. 2002. Influence of harvest date and light integral on the development of strawberry flavour compounds. *J Exp Bot.* 53(377):2121–2129. <https://doi.org/10.1093/jxb/erf088>.
- Yamaki S. 2010. Metabolism and accumulation of sugars translocated to fruit and their regulation. *J Japan Soc Hort Sci.* 79(1):1–15. <https://doi.org/10.2503/jjshs.1.79.1>.
- Zhang Y, Hu W, Peng X, Sun B, Wang X, Tang H. 2018. Characterization of anthocyanin and proanthocyanidin biosynthesis in two strawberry genotypes during fruit development in response to different light qualities. *J Photochem Photobiol B.* 186:225–231. <https://doi.org/10.1016/j.jphotobiol.2018.07.024>.
- Zhu J, Génard M, Poni S, Gambetta GA, Vivin P, Vercambre G, Trought MCT, Ollat N, Delrot S, Dai Z. 2019. Modelling grape growth in relation to whole-plant carbon and water fluxes. *J Exp Bot.* 70(9):2505–2521. <https://doi.org/10.1093/jxb/ery367>.